Osteolytic disease in IL-6 and Myc dependent mouse model of human myeloma

Focal and generalized bone loss is a hallmark of multiple myeloma (MM) that is poorly recapitulated in genetically engineered mouse models (GEMM) of myeloma development. To address this shortcoming, we used integrated whole-body *ex vivo* X-ray microscopy and micro-computed tomography (μCT) to evaluate skeletal decay in primary plasma cell tumor (PCT)-bearing IL6Myc mice, a model system of neoplastic plasma cell development driven by transgenic expression of human IL-6 and mouse MYC. Skeletal changes mimicking human myeloma bone disease (MBD) were detected in 10 of 10 randomly chosen IL6Myc mice carrying advanced PCT. MBD-like disease was more pronounced in long bones than the axial skeleton or skull; was caused, at least in part, by increased osteoclast-dependent bone resorption that led to heightened secretion of tartrate-resistant acid phosphatase (TRAP); was associated with elevated serum levels of receptor activator of nuclear factor kappa-B ligand (RANKL) and reduced levels of its decoy receptor, osteoprotegerin (OPG); and was accompanied by a rise in IL-17 producing T-helper cells in the bone marrow. These findings complemented our previous work on the utility of *in vivo* ^{18}F-fluorodeoxyglu-

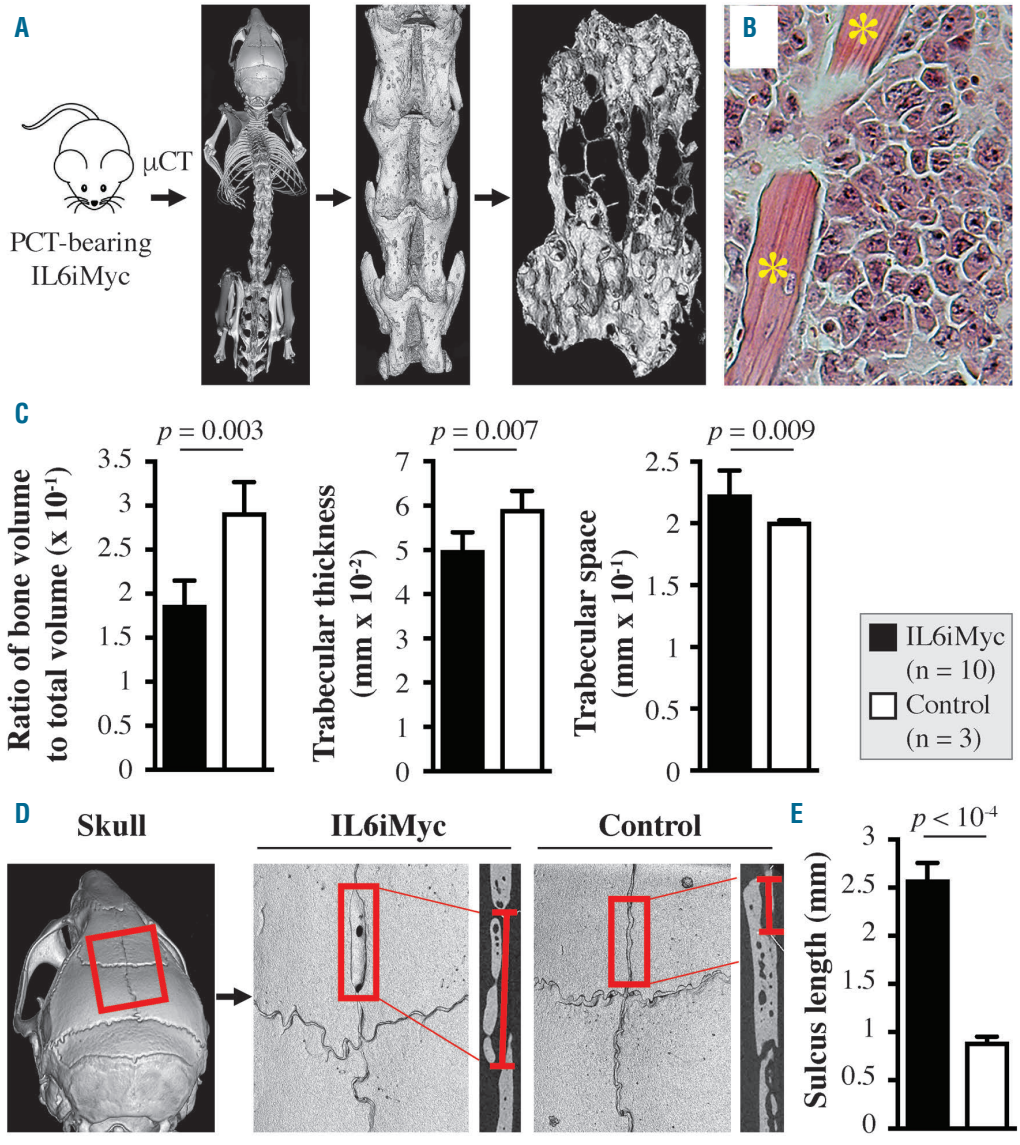

Figure 1. Moderate bone loss in the spinal column of tumor-bearing IL6Myc mice. (A) 3D μCT images of the central skeleton of a tumor-bearing IL6Myc mouse at 50 μm² resolution (left panel), L2-4 at 8 μm² resolution (center) and the L2 bone cylinder used for quantitative determination of bone mass (right). IL6Myc mice carry human IL-6 and mouse Myc (c-myc) encoding transgenes on the genetic background of BALB/c (C). The transgenes cooperate to drive neoplastic plasma cell development with full genetic penetrance (100% tumor incidence) and short tumor onset (4-5 months). (B) Photomicrograph of a PCT infiltrating the lumbar spine. The tissue section was stained with hematoxylin and eosin (H&E; original magnification 63x). Trabecular bone (indicated by yellow asterisks) has been eroded by the malignant plasma cells. (C) Bar diagrams comparing BV/TV (left), Tb.Th (center) and Tb.Sp (right) in 10 PCT-carrying transgenic mice (five males and five females) at 4-5 months of age (black bars) and three age-matched normal C mice (two males and one female; white bars). (D) 3D X-ray image of a mouse cranium consisting of bone plates held together by several transverse, ossified sutures and one median (sagittal) suture (left panel). Elongated sulcus-like gap in the sagittal suture of a tumor-bearing mouse relative to a normal mouse (center panel). The length of the gap was measured in both groups of mice and used for statistical comparison in panel E. (E) Bar diagram of changes described in panel D indicative of sagittal suture erosion in tumor-bearing mice.

cose positron emission tomography (FDG-PET) imaging in the IL6Myc model[1] and suggested that the model lends itself to studies on the natural history of MBD and the development of new approaches to its treatment and prevention.

In addition to constituting a disease-defining feature with major contributions to morbidity, MBD increases the treatment cost and lessens the quality of life of patients with myeloma.[2] This is due to focal bone loss that affects the axial skeleton and proximal long bones causing severe pain, pathological fractures, instability of the vertebral column, and medullary cord or spinal nerve root compression – among a host of other complications collectively referred to as skeletal-related events. Treatment for MBD including drugs, radiotherapy, and surgery is available, but is often less than effective[3] despite advances in understanding the pathophysiology of MBD and a busy drug development pipeline.[4] The circumstance that the majority of myeloma patients develop osteolytic lesions (~85%) in the course of myeloma treatment underlines that MBD is an unmet medical need that warrants additional research including fundamental preclinical studies.[5] To that end, a number of mouse models are available,[6] although none are perfect. The most

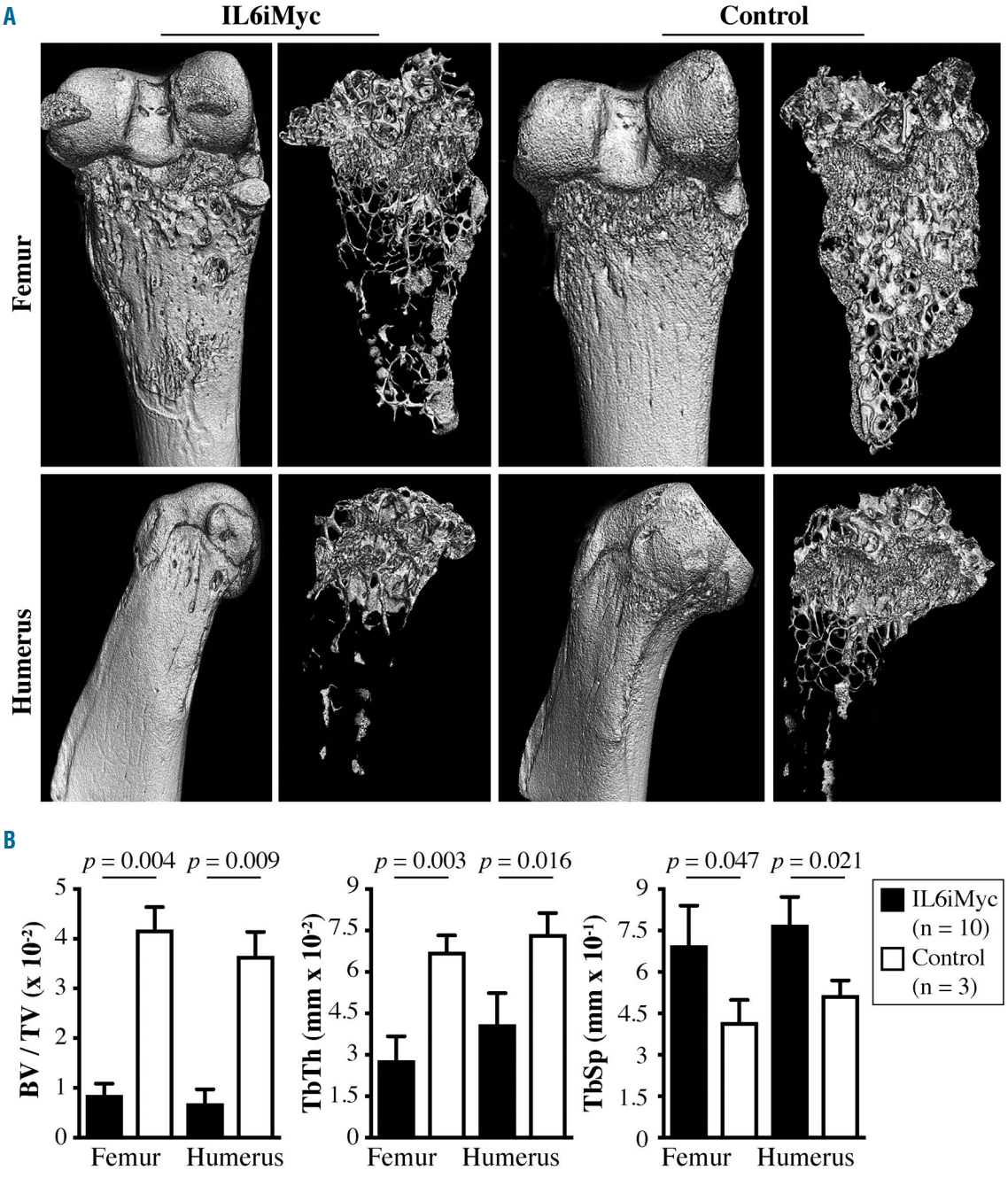

Figure 2. Significant bone loss in long bones of tumor-bearing IL6Myc mice. (A) 3D rendering of μCT images of proximal femur (top row) and humerus (bottom row) samples obtained from tumor-bearing IL6Myc mice (left) or controls (right). (B) Bar diagrams of BV/TV (left), Tb.Th (center) and Tb.Sp (right) in tumor-bearing (black) and normal (white) mice. Mean values are plotted and the standard deviation (SD) are indicated by short vertical lines.

widely used models, which rely on the propagation of either human myeloma cells in immunodeficient hosts[7] or myeloma-like mouse cells in immunocompetent hosts,[8,9] are hampered by the reality that *in vivo* transfer of fully transformed tumor cells is not suitable for evaluating bone loss that slowly accumulates in the course of primary tumor development. Genetically engineered mice wherein PCT arise *de novo* may fill this gap, but the evidence for MBD-like changes in these mice are usually limited to "representative" X-ray or μCT images that merely indicate osteolytic disease may occur.

To assess the incidence, severity and reproducibility of MBD-like changes in the IL6Myc model in an objective and quantitative manner, we took advantage of high-resolution 3D X-ray imaging and μCT analysis (8 μm^2 pixel size) to survey 10 tumor-bearing mice exhibiting hind

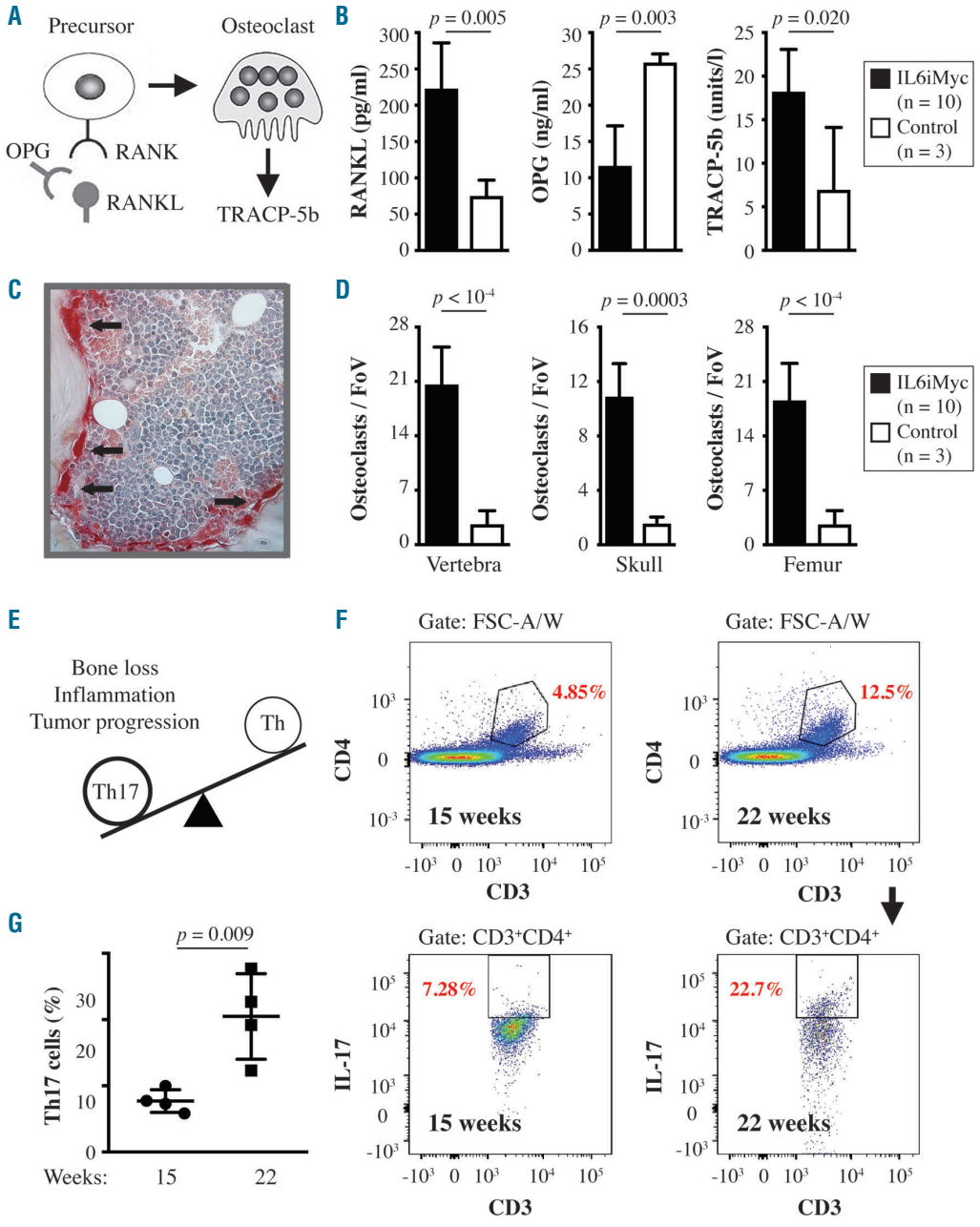

Figure 3. Elevated osteoclast-dependent bone resorption and increased abundance of bone marrow Th17 cells. (A) Osteoclast development scheme. RANK is expressed on osteoclast precursors. Binding of its ligand, RANKL, either in soluble form or on cell surfaces, promotes osteoclast differentiation. The decoy receptor, OPG, inhibits the interaction of RANK and RANKL and, therefore, suppresses osteoclast development. TRAP (TRACP-5b) is a biomarker of osteoclast development and activation. (B) Bar graphs of RANKL, OPG and TRACP-5b serum levels in tumor-bearing (black) and normal (white) mice. Mean values and SDs are plotted. Results of *t* tests are indicated by horizontal lines that are labeled. (C) Detection of TRAP⁺ osteoclasts (dark red cytoplasm) in immunostained tissue sections of vertebral bone harvested from a PCT-bearing IL6Myc mouse. (D) Column diagrams of mean TRAP⁺ osteoclast numbers per field of view. Osteoclasts were enumerated in tissue sections like the one shown in panel C. (E) Scheme indicating that a skew of bone marrow infiltrating helper T cells to Th17 has been implicated in MBD. (F) Flow cytometric determination of IL-17 producing $CD3^+CD4^+$ T helper cells in the bone marrow. T-helper cells histograms (upper panels) and Th17 cells (lower panel) are shown. Mice 15 and 22 weeks of age are presented to the left and right, respectively. (G) Abundance of Th17 cells in the bone marrow of 15-week-old mice (n=4) and 22-week-old mice (n=4).

limb weakness and incipient paraplegia. Lumbar vertebrae 2, 3 and 4 (L2–4) were used as indicator bones and whole-skeleton 3D X-ray imaging at low resolution of 50 μm^2 was carried out prior for orientation and overview (Figure 1A). 3D rendering of stacked 8 μm^2 images revealed a moderate but significant amount of bone loss consequent to malignant intramedullary plasma cell growth (Figure 1B). Bone loss took the form of thinning and perforation of cortical bone and diminution of cancellous, spongy bone. Histomorphometric µCT analysis, using BoneJ as a software tool, demonstrated a decline (P=3x10^{-4}) in the mean bone volume (measured as the ratio of bone volume to tissue volume: BV/TV) of IL6Myc mice relative to age-matched BALB/c mice used as control (Figure 1C, left). Consistent with the significant but moderate loss of bone volume, mean trabecular thickness (Tb.Th) was moderately reduced (15%, P=0.0073, Figure 1C, center) and mean trabecular space was moderately increased (11%, P=0.0085; Figure 1C, right) in tumor-bearing mice. Image analysis of the cranium (Figure 1D) demonstrated a substantial weakening and erosion of the coronal, sagittal and lambdoidal sutures in IL6Myc. This resulted in a sulcus-like gap anterior to the sagittal suture, the length of which correlated with the severity of bone loss: on average, IL6Myc mice exhibited a ~3-fold increase compared to controls (P<10^{-4}; Figure 1E).

To follow up on the findings described above, we performed high-resolution µCT imaging of proximal long bones in PCT-bearing IL6Myc mice (Figure 2A). Relative to controls, the mean volume of the proximal femur and humerus was strikingly reduced in tumor-carrying mice, by ~80% in both cases (Figure 2B, left). Trabecular thickness and space changed accordingly; *i.e.*, the thickness in the femurs and humeri of IL6Myc mice was reduced by 59% and 44%, respectively (Figure 2B, center) whereas the trabecular space was increased by 67% in femurs and 50% in humeri (Figure 2B, right). The substantial bone loss seen in PCT-bearing mice raised the question whether the RANK/RANKL axis might be mechanistically involved. This axis is crucial for the natural history of MBD and provides the molecular target for the RANKL-inhibiting antibody, denosumab, in myeloma therapy 10. Figure 3A shows that binding of RANKL to RANK (expressed on osteoclast precursors) promotes osteoclast development, whereas the RANKL decoy receptor, OPG, has the opposite effect.

To evaluate whether tumor-bearing IL6Myc mice demonstrate changes in serum levels consistent with elevated osteoclast-dependent bone resorption, we used ELISA to determine soluble RANKL and OPG. Compared to normal BALB/c mice, RANKL was 3-fold increased (Figure 3B, left) and OPG was 2.2-fold decreased (Figure 3B, center) in IL6Myc mice. In line with the shifted RANKL-to-OPG ratio, tartrate-resistant acid phosphatase (TRAP, a.k.a. acid phosphatase 5, tartrate resistant or TRACP-5b), a biomarker of osteoclast activation, was significantly elevated (2.6-fold) in IL6Myc mice relative to controls (Figure 3B, right). These results were confirmed by the enumeration of $TRAP^+$ osteoclasts in immunostained bone sections of PCT-bearing IL6Myc mice (Figure 3C). Osteoclasts were more abundant in three different anatomical sites – vertebrae, femur and cranium (Figure 3D) – indicating osteolytic damage occurs systemically in tumor-laden mice.

Research by other investigators has shown that the abundance of pro-inflammatory Th17 cells governs, in part, the cytotoxic immune response in myeloma[11] and that targeting Th17 cells may afford a new treatment approach to MBD[12] (Figure 3E). Additionally, a recent study using the Vκ*MYC model of human myeloma provided definitive evidence that Th17 cells are able to accelerate neoplastic plasma cell development.[13] To assess whether increased bone marrow Th17 cells is a feature of MBD-like disease in tumor-bearing IL6Myc mice, we performed a pilot experiment comparing four 15-week-old mice at an early tumor stage with four 22-week-old mice harboring frank neoplasms. Th17 cells were enumerated as IL-17 producing $CD3^+CD4^+$ T-helper cells (Figure 3F). The mean abundance of Th17 cells in 22-week-old mice (20.5%) was more than twice as high (P= 0.009) than in the 15-week-old mice (7.71%, Figure 3G). The variability in the advanced tumor group was high, possibly due to differences in bone marrow plasma levels of IL-6 which promotes Th17 but suppresses Treg differentiation.[14] Although preliminary, the findings suggested that IL-17 plays a role in MBD-like disease in the IL6Myc model, just as it does in human MBD.

In conclusion, the main finding of this study is the pronounced proclivity of IL6Myc mice to MBD-like disease. Bone loss occurred in a host environment that contains a fully intact innate and adaptive immune system, rendering the mouse model potentially useful for translational studies on myeloma immunotherapy, a growth area in the clinic that includes promising trials on MBD.[15] Another strength of IL6Myc is the ability to integrate *in vivo* whole-body FDG-PET imaging[1] with targeted *ex vivo* µCT analysis. This may permit comparisons of the impact of experimental MBD therapies on bone status and lesion repair, on the one hand, and metabolic activity of neoplastic plasma cells, on the other. Finally, an important practical consideration for assessing preclinical drug effects concerns the requirement for a sufficiently large therapeutic window from the commencement of treatment at the onset of osteolytic disease to the evaluation of treatment responses at the end stage. In IL6Myc mice this window is likely wide enough, as demonstrated by a pilot treatment study using the second-generation proteasome inhibitor ixazomib.[1]

Fumou Sun,[1] Yan Cheng,[1] Susan A. Walsh,[2] Michael R. Acevedo,[2] Xuefang Jing,[3] Seong Su Han,[4] Michael D. Pisano,[1,5] Michael H. Tomasson,[6,7] Alan K. Lichtenstein,[8] Fenghuang Zhan,[6,7] Parameswaran Hari[4,9] and Siegfried Janz[1,9]

[1]Division of Hematology and Oncology, Department of Medicine, Medical College of Wisconsin, Milwaukee, WI; [2]Department of Radiology, Medical College of Wisconsin, Milwaukee, WI; [3]Department of Pathology, Medical College of Wisconsin, Milwaukee, WI; [4]Department of Pediatrics, Medical College of Wisconsin, Milwaukee, WI; [5]Interdisciplinary Graduate Program in Immunology, The University of Iowa Roy J. and Lucille A. Carver College of Medicine, Iowa City, IA; [6]Internal Medicine, The University of Iowa Roy J. and Lucille A. Carver College of Medicine, Iowa City, IA; [7]Holden Comprehensive Cancer Center, The University of Iowa Roy J. and Lucille A. Carver College of Medicine, Iowa City, IA; [8]Department of Hematology-Oncology, University of California at Los Angeles, Los Angeles, CA and [9]Cancer Center, Medical College of Wisconsin, Milwaukee, Wisconsin, USA

FS and YC are co-first authors.

Funding: this work was supported in part by the MCW Milwaukee William G. Schuett, Jr., Multiple Myeloma Research Endowment; NCI Core Grant P30CA086862 in support of The University of Iowa Holden Comprehensive Cancer Center; National Natural Science Foundation of China (NNSFC) Award 81228016 (to FZ); and NCI R01CA151354 (to SJ).

Correspondence: SIEGFRIED JANZ.
sjanz@mcw.edu

doi:10.3324/haematol.2019.221127

Information on authorship, contributions, and financial & other disclosures was provided by the authors and is available with the online version of this article at www.haematologica.org.

References

1. Duncan K, Rosean TR, Tompkins VS, et al. (18)F-FDG-PET/CT imaging in an IL-6- and MYC-driven mouse model of human multiple myeloma affords objective evaluation of plasma cell tumor progression and therapeutic response to the proteasome inhibitor ixazomib. Blood Cancer J. 2013;3:e165.
2. Bingham N, Reale A, Spencer A. An evidence-based approach to myeloma bone disease. Curr Hematol Malig Rep. 2017;12(2):109-118.
3. Ring ES, Lawson MA, Snowden JA, Jolley I, Chantry AD. New agents in the treatment of myeloma bone disease. Calcif Tissue Int. 2018;102(2):196-209.
4. Terpos E, Ntanasis-Stathopoulos I, Gavriatopoulou M, Dimopoulos MA. Pathogenesis of bone disease in multiple myeloma: from bench to bedside. Blood Cancer J. 2018;8(1):7.
5. Silbermann R, Roodman GD. Current controversies in the management of myeloma bone disease. J Cell Physiol. 2016; 231(11):2374-2379.
6. Lwin ST, Edwards CM, Silbermann R. Preclinical animal models of multiple myeloma. Bonekey Rep. 2016;5:772.
7. Yaccoby S, Barlogie B, Epstein J. Primary myeloma cells growing in SCID-hu mice: a model for studying the biology and treatment of myeloma and its manifestations. Blood. 1998;92(8):2908-2913.
8. Radl J, Croese JW, Zurcher C, Van den Enden-Vieveen MH, de Leeuw AM. Animal model of human disease. Multiple myeloma. Am J Pathol. 1988;132(3):593-597.
9. Hofgaard PO, Jodal HC, Bommert K, et al. A novel mouse model for multiple myeloma (MOPC315.BM) that allows noninvasive spatiotemporal detection of osteolytic disease. PLoS One. 2012;7(12):e51892.
10. Raje NS, Bhatta S, Terpos E. Role of the RANK/RANKL pathway in multiple myeloma. Clin Cancer Res. 2019;25(1):12-20.
11. Marino S, Roodman GD. Multiple myeloma and bone: the fatal interaction. Cold Spring Harb Perspect Med. 2018;8(8).
12. Prabhala RH, Fulciniti M, Pelluru D, et al. Targeting IL-17A in multiple myeloma: a potential novel therapeutic approach in myeloma. Leukemia. 2016;30(2):379-389.
13. Calcinotto A, Brevi A, Chesi M, et al. Microbiota-driven interleukin-17-producing cells and eosinophils synergize to accelerate multiple myeloma progression. Nat Commun. 2018;9(1):4832.
14. Zhou L, Ivanov, II, Spolski R, et al. IL-6 programs T(H)-17 cell differentiation by promoting sequential engagement of the IL-21 and IL-23 pathways. Nat Immunol. 2007;8(9):967-974.
15. Raje N, Terpos E, Willenbacher W, et al. Denosumab versus zoledronic acid in bone disease treatment of newly diagnosed multiple myeloma: an international, double-blind, double-dummy, randomised, controlled, phase 3 study. Lancet Oncol. 2018;19(3):370-381.